JOURNAL OF MATERIALS SCIENCE 18 (1983) 669–678

Sintering Al_2O_3–B_4C ceramics

K. C. RADFORD
Nuclear Materials Department, Westinghouse Research and Development Center, Pittsburgh, Pennsylvania 15235, USA

Microstructural development of Al_2O_3–B_4C composite ceramics has been studied as a function of Al_2O_3 and B_4C powder types, and also in various sintering atmospheres. Boron carbide suppresses the sinterability of Al_2O_3 powder, and the densification of the composite is strongly dependent on both B_4C and Al_2O_3 properties. Temperatures $\geqslant 1700^\circ$ C cause significant increases in sintering kinetics.

1. Introduction

Boron is particularly attractive for reactivity control of nuclear reactors because of the high cross-section of the ^{10}B isotope. The most extensive use has been in the form of the carbide, B_4C, owing to its low cost and ease of fabrication, and for burnable absorber applications dilution of the ^{10}B atoms either by depletion (^{10}B isotope separation) or by dispersion in an inert matrix is generally required. For economic reasons, dilution in a ceramic matrix, such as Al_2O_3, SiO_2 or SiC is preferred. Whereas Al_2O_3–B_4C has been fabricated and irradiated on a number of occasions [1, 2], and is currently used in commercial power reactors, little information is available on the sintering and properties of the material. Because the current trend for nuclear power generation is to improve uranium utilization by extending reactor reload cycles and increasing fuel burn-ups, interest in Al_2O_3–B_4C composites for burnable absorber applications prompted a study of the system in order that the changes in material properties due to variability in the manufacturing process could be understood, and the effects on reactor performance evaluated.

2. Experimental procedure

Fabrication of Al_2O_3–B_4C composite pellets was studied using five B_4C and ten Al_2O_3 powders having different physical characteristics. The B_4C powders were nuclear grade and the Al_2O_3 powders included a variety of low-cost Alcoa and Reynolds commercial grades, and the more expensive very active Linde A and fused-grain Norton materials.

Examination of the powders included particle-size distributions and BET surface areas, with the results as listed in Table I, and also replica transmission electron microscopy of the four Al_2O_3 powders having the highest surface areas. The particle-size distributions of the Al_2O_3 powders were obtained using a Micromeritics Particle Size Analyzer*, and the B_4C distributions with a Leitz Classimat† using powder dispersed on a glass slide.

Compositions were made by ball milling the materials in deionized water for 2 h, with the addition of dispersing agents and binders (carbowax and PVA). The powders were air dried with stirring (some compositions were spray dried), sieved through a 100 mesh screen and pellets pressed isostatically at 30×10^3 psi.‡ The pellets were dewaxed in a vacuum of about 1×10^{-6} torr at 500° C prior to sintering in graphite boats. Sintering was performed in an Al_2O_3 muffle, molybdenum element furnace except for the vacuum experiments which used a tantalum element, cold-wall furnace. The investigations involved temperatures from 1300 to 1800° C and a variety of atmospheres, including nitrogen, argon, hydrogen and vacuum.

The sintered pellet densities were established by water immersion with at least five samples

*Micromeritics Instrument Corp, Norcross, Georgia, USA.
†E. Leitz Inc., Rockleigh, New Jersey, USA.
‡1 psi = 6.894×10^3 Pa

0022–2461/83/030669–10$03.70/0

TABLE I Physical Properties of Al_2O_3 and B_4C powders

Alumina	Surface area ($m^2\ g^{-1}$)	Particle size (μm)			Boron carbide	Surface area ($m^2\ g^{-1}$)	Particle size (μm)		
		Mean	Max	Min			Mean	Max	Min
1. Alcoa A14-325	0.84	5.90	30	3.20	A. Atomergic-100 Mesh	0.54	38.00	80	2.00
2. Alcoa A15-325	5.01	2.75	30	0.90	B. Atomergic-1000 Mesh	2.71	11.00	15	0.70
3. Alcoa A15-SG	4.57	2.43	20	1.30	C. Norton	4.25	12.00	38	1.00
4. Alcoa A16-SG	11.30	1.00	11	0.10	D. Carborundum	21.80	2.40	28	0.10
5. Reynolds RC-HP	2.79	8.20	40	2.50	E. Tetrabor	38.93	0.28	6	0.09
6. Reynolds RC-HPT-DBM	4.30	0.84	15	0.13					
7. Reynolds RC-172-DBM	5.21	0.67	11	0.10					
8. Reynolds RC-HP-DBM	7.95	0.43	9	0.10					
9. Linde A	13.80	0.96	25	0.20					
10. Norton 38 Alundum-1200	12.87	1.55	7	0.32					

per composition. The pellets were sectioned and examined metallographically using standard preparation techniques, and several pellets were studied for chemical interactions using Auger spectroscopy and electron microprobe methods.

3. Results

B_4C is an effective sintering inhibitor for Al_2O_3 as seen in Fig. 1. Microstructural examination indicated that the B_4C particles are not measurably changed in size during sintering and do not appear to participate in the sintering process. Consolidation of the sample occurs by densification of the Al_2O_3 matrix, but unlike the pure Al_2O_3 samples, which sinter to $>90\%$ theoretical density (TD) at $\sim 1500^\circ$ C, the composite samples suffer a significant reduction in density with only a very small addition of B_4C, and the microstructure contains a substantial quantity of fine porosity on the order of 1 μm. Little further decrease in density is obser-

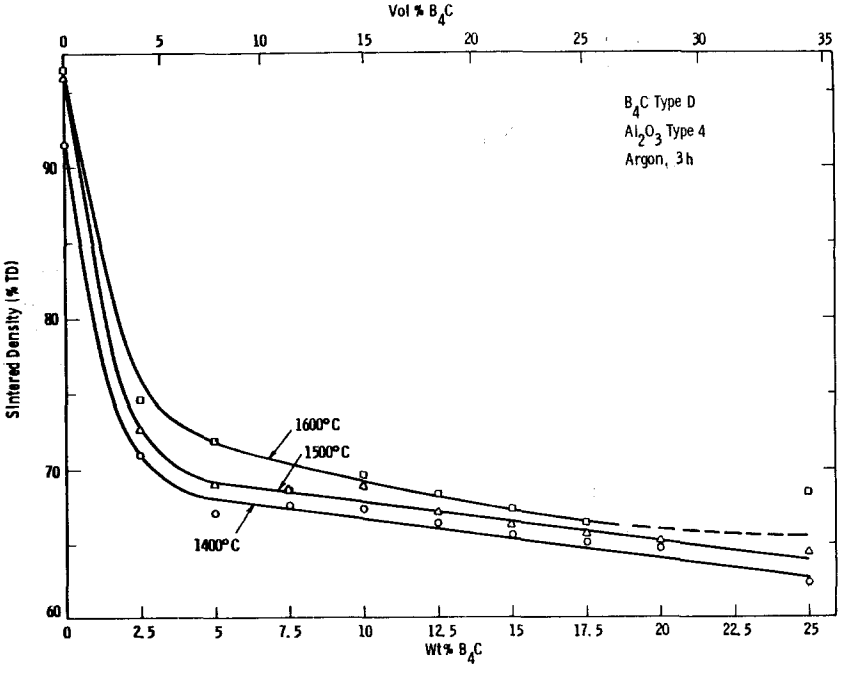

Figure 1 Effect of B_4C loading on the sinterability of Al_2O_3–B_4C.

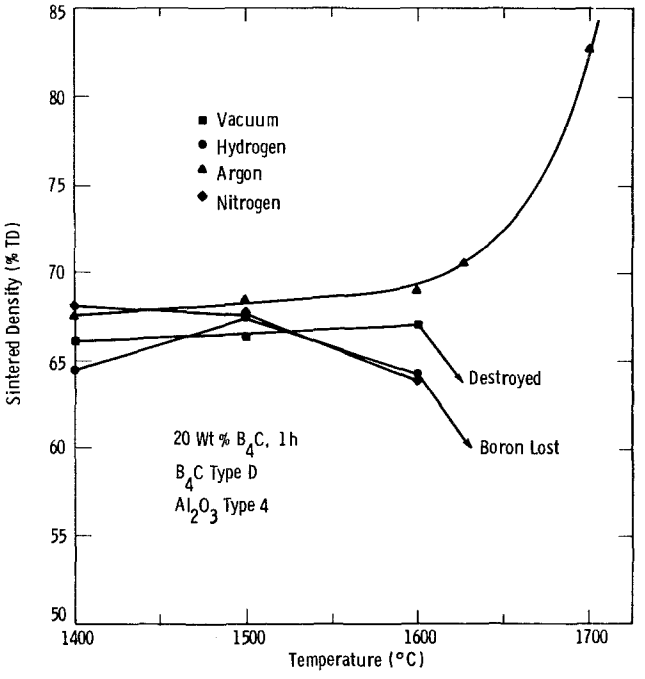

Figure 2 Effect of atmosphere on the sintered density of Al_2O_3–B_4C.

ved with increase in the B_4C level beyond about 5 wt %. It can also be seen in Fig. 1 that temperatures in the range 1400 to 1600° C do not have a large effect on densification. However, as seen in Fig. 2, temperatures in excess of 1600° C cause a very rapid increase in density. This increase in density is only observed in argon and sintering in other atmospheres shows mixed results. Vacuum is effective up to 1600° C, although the sintered density is lower than for argon, but complete deterioration through reaction induced evaporation of the sample occurs at higher temperatures. Contrary to reported information [1], sintering in dry hydrogen does not produce good sintered samples; optimum temperature for H_2 sintering is 1500° C, above which boron loss is observed. A similar effect is noted using nitrogen which produces the highest sintered density at 1400° C, but progressively lower densities with increase in temperature.

Boron loss occurred under all sintering conditions as seen in Fig. 3 for argon and nitrogen atmospheres. A gradual loss with increase in sintering temperature is seen for argon, whereas a precipitous drop above 1400° C is found with nitrogen.

Sintering time (Fig. 4) does not have an appreciable effect at temperatues of 1500° C or below. At higher temperatures extended soak times result

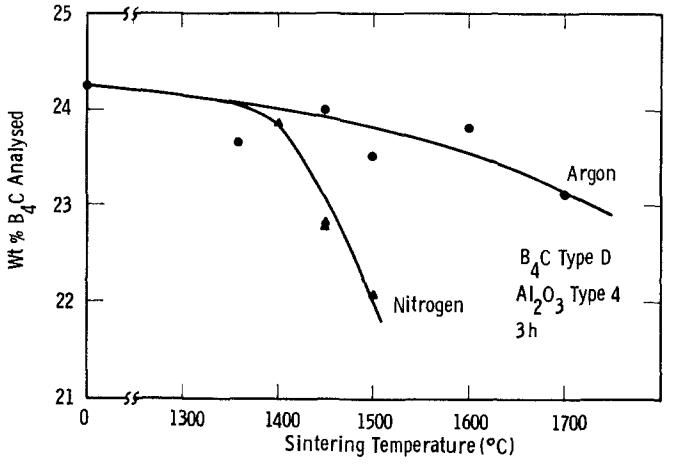

Figure 3 Analysed B_4C content of Al_2O_3–B_4C pellets sintered at different temperatures in nitrogen and argon atmospheres.

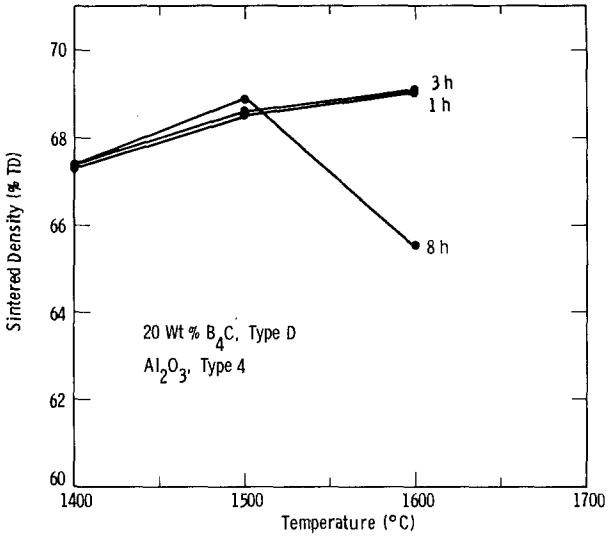

Figure 4 Effect of soak time in argon on the sintered density of Al_2O_3–B_4C pellets.

in density reductions and enhanced boron loss. The surface area of the B_4C powder has a marked effect on pellet densification. A very good correlation between density (ρ) and surface area (SA) was observed as seen in Fig. 5, giving a $\rho \propto SA^{-0.03}$ dependence, indicating that greater surface area of B_4C results in lower sintered densities. The identities of the points correspond to those of Table I.

In contrast, the sintered densities of the samples were found to depend primarily on the median particle size (d) of the Al_2O_3 powder, as seen in Fig. 6, with a $\rho \propto d^{-0.14}$ relationship. Higher densities were obtained with finer Al_2O_3 powders. Correlations with surface areas, Fig. 7a, showed separate relationships depending on the powder types. For 14 wt% B_4C powder, the Alcoa powders (nos. 1 to 4) showed a more gradual increase in sintered density with increase in Al_2O_3 surface area than the Reynolds powders (nos. 5 to 7). For a 20 wt% loading of finer B_4C powder (Fig. 7b) the influence of Al_2O_3 powder activity was apparent, but the differences previously observed due to powder type were not seen.

Microstructural evaluation of the various powders showed results consistent with the sintered densities, and differences due to variations in properties of the Al_2O_3 and B_4C powders. Some representative micrographs for samples sintered for 3 h in argon at 1500° C are shown in Fig. 8 which highlight the important features of the sintering process. The appearance of Sample 8a containing the fine Carborundum B_4C and the highly sinterable Alcoa A16SG powder shows evidence of the individual Al_2O_3 powder particles, indicating that the sample is not fully sintered. In contrast, using the same Al_2O_3 powder but coarser Norton B_4C powder (Fig. 8b), a more sintered Al_2O_3 matrix is obtained although considerable fine ($\sim 1\,\mu m$) porosity is evident as well as the coarse ($> 10\,\mu m$) pores that are normally observed in most samples, and implying

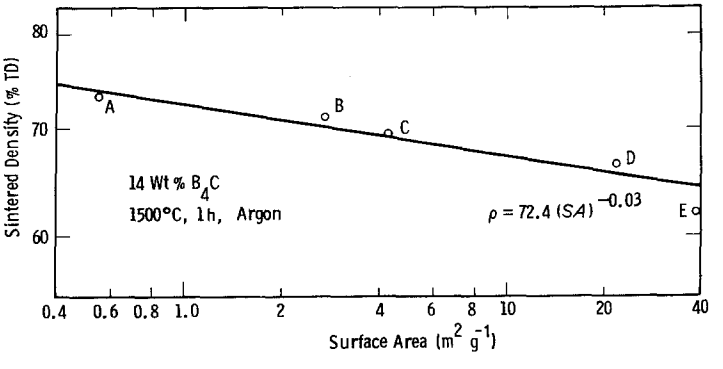

Figure 5 Effect of B_4C surface area on sintered density of type 4 Al_2O_3 powder.

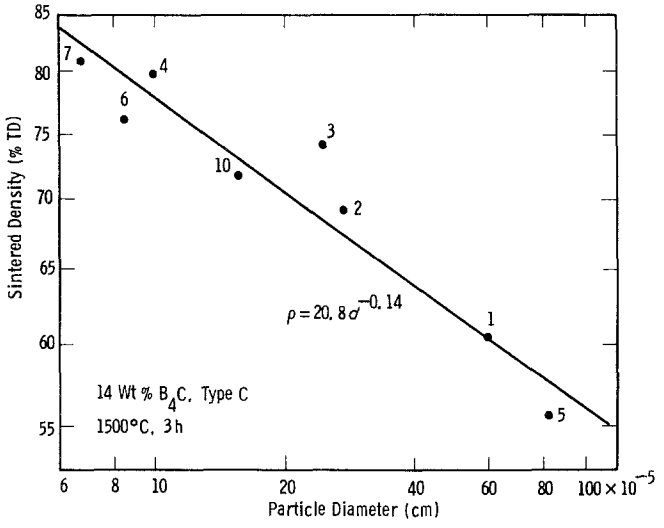

Figure 6 Dependence of sintered density on particle size of Al_2O_3 powder.

that whatever inhibits sintering is less pronounced with this coarser grade B_4C. Sample 8c shows the highest matrix density and fewer coarse pores obtained using the same B_4C powder in Reynolds RC172 Al_2O_3, while in Fig. 8d the fused grain, Norton 38 Alundum 1200 Al_2O_3 with the Norton B_4C shows the individual Al_2O_3 crystallites indicating poorer interparticle sinterability than the Alcoa and Reynolds powders even though the initial surface area was higher.

Although densities below theoretical were obtained with B_4C additions > 5 wt %, and the majority of samples were below 80% TD, higher densities were obtained under certain conditions.

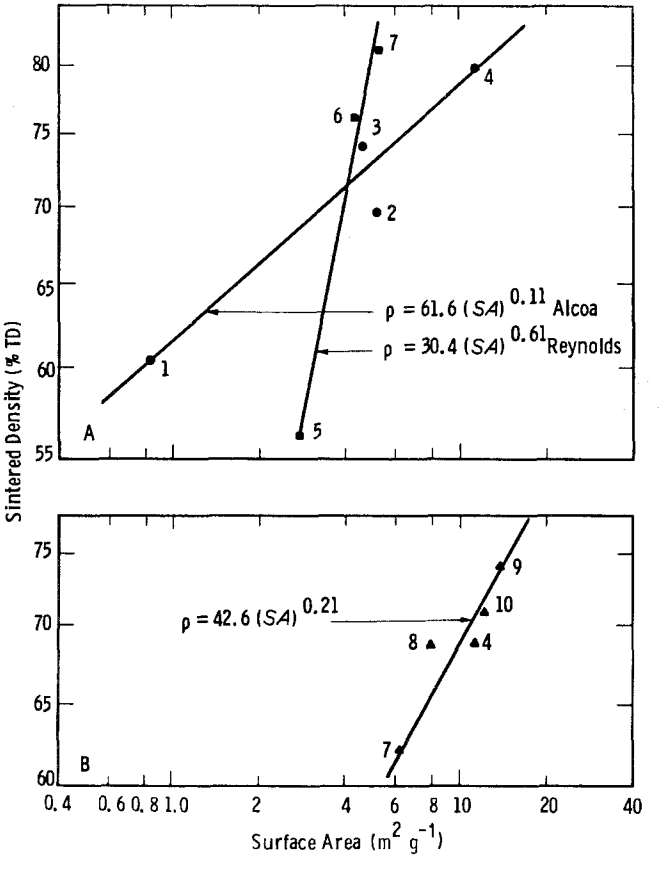

Figure 7 Dependence of sintered density on Al_2O_3 powder surface area: (a) for 14 wt % B_4C, type C; (b) for 20 wt % B_4C, type D.

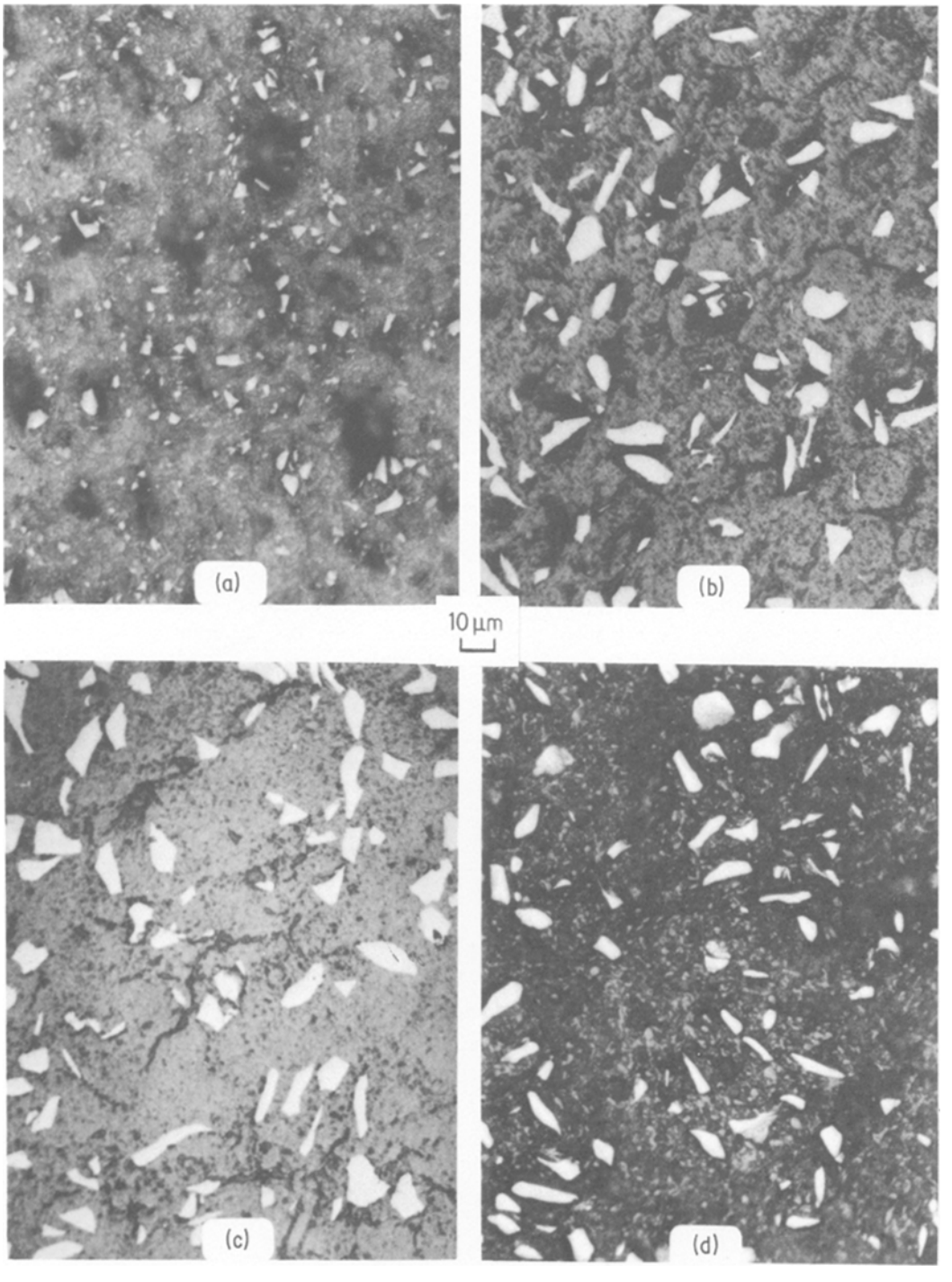

Figure 8 Microstructures of typical Al_2O_3–B_4C compositions sintered for 3 h at 1500° C in argon. (a) B_4C powder D in Al_2O_3 powder 4 giving a structure with significant very fine porosity. (b) B_4C powder C with same Al_2O_3 producing a more sintered structure with somewhat coarser pores. (c) B_4C powder C with Al_2O_3 powder 7 producing a high-density matrix. (d) B_4C powder C with Al_2O_3 powder 10 showing a poorly sintered structure with individual particles evident.

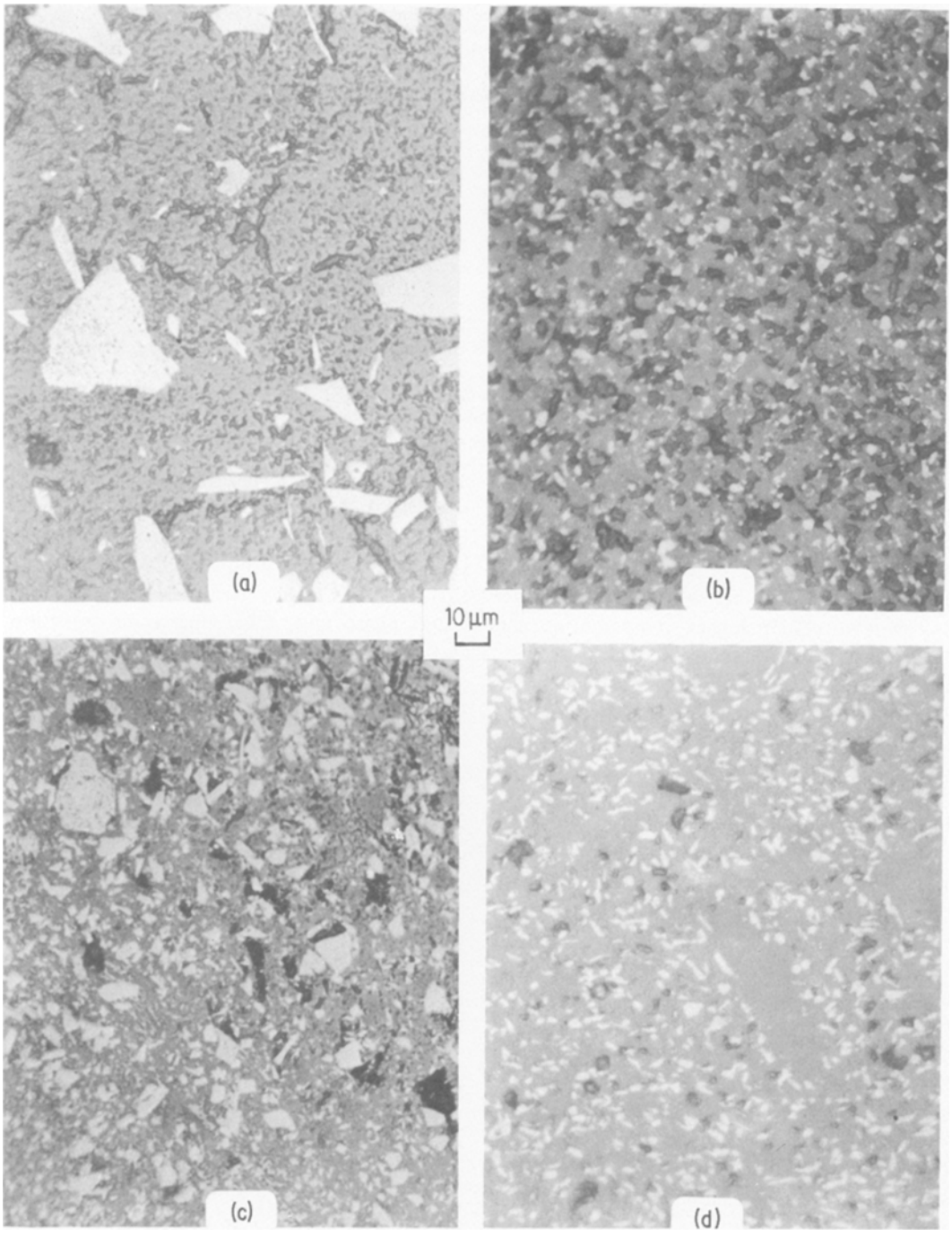

Figure 9 Influence of powder type and temperature on resulting Al_2O_3–B_4C microstructure. (a) B_4C powder A with Al_2O_3 powder 4 sintered to 80% TD at 1500° C; (b) B_4C powder B with Al_2O_3 powder 9 sintered to 82% TD at 1600° C; (c) B_4C powder D with Al_2O_3 powder 4 sintered to 85% TD at 1700° C; (d) B_4C powder E with Al_2O_3 powder 9 sintered to 92% TD at 1800° C.

TABLE II Free energy changes (cal* mol^{-1}) for possible reactions for Al_2O_3–B_4C composites

Reaction		Temperature (K)			Comments
		1700	1800	1900	
$B_4C + 2N_2 \rightarrow 4\,BN + C$	(1)	−89181	−81087	−72998	Will occur
$B_4C + 2N_2 \rightarrow 4\,BN + CH_4$	(2)	+30956	+33431	+35900	No reaction
$B_4C + 4H_2O \rightarrow 4\,BO + 4H_2 + C$	(3)	−1916	−15524	−29088	Will occur
$Al_2O_3 + N_2 \rightarrow 2\,AlN + 3/2\,O_2$	(4)	+208256	+206080	+203926	No reaction
$Al_2O_3 + 2H_2 \rightarrow Al_2O + 2\,H_2O$	(5)	+136742	+130784	+124891	No reaction
$Al_2O_3 + H_2 \rightarrow Al_2O_2 + H_2O$	(6)	+146633	+141532	+136485	No reaction
$Al_2O_3 + C \rightarrow Al_2O_3 + CO$	(7)	+120532	+112052	+103521	No reaction
$Al_2O_3 + B_4C \rightarrow 2\,AlB_2 + CO + O_2$	(8)	Positive	Positive	Positive	No reaction
$2\,Al_2O_3 + 3B_4C \rightarrow Al_4C_3 + 6B_2O$	(9)	+421779	+394793	+367994	No reaction
$Al_2O + B_4C \rightarrow 2\,AlB_2 + CO$	(10)	Negative	Negative	Negative	Will occur
$Al_2O_2 + B_4C \rightarrow 2\,AlB_2 + CO_2$	(11)	Negative	Negative	Negative	Will occur

Thermodynamic properties of aluminium borides have not been found, but for Equations 10 and 11, a free energy of formation > -5900 cal mol^{-1} for AlB_2 at 1700 K will cause reaction to occur; although AlB_2 is not expected to be very stable, this value appears reasonable. Reaction 8 will not occur.

*1 cal = 4.184 J

Coarse B_4C powders, such as type A, enable relatively high densities (80% + TD) to be fabricated at temperatures below 1600° C but finer B_4C powders require higher temperatures and Al_2O_3 powders with reasonable activities (i.e., surface areas $> 4\,m^2\,g^{-1}$) to obtain densities $\geqslant$ 80% TD. Some representative structures are seen in Fig. 9.

Fig. 9a shows a pellet of ~ 80% TD sintered at 1500° C using coarse B_4C powder (type A) with Alcoa A16 Al_2O_3 in which the majority of the porosity is fine, and few coarse pores are evident. With increase in temperature, fine B_4C can be sintered to high density as typified by Fig. 9b for Linde A with type B B_4C sintered at 1600° C to 82% TD. Fig. 9c shows the broad distribution B_4C powder type D in an A16 Al_2O_3 matrix with a density of 85% TD obtained by sintering at 1700° C, and Fig. 9d shows a pellet with the fine type E B_4C and Linde A Al_2O_3 sintered at 1800° C to a density of 92% TD.

4. Discussion

Apart from the sintering temperature and furnace atmosphere, sinterability of Al_2O_3–B_4C composites is strongly dependent on the properties of the Al_2O_3 powder as well as on the properties of the B_4C powder. The more active, finer Al_2O_3 powders produce higher sintered densities, whereas the finer B_4C powders cause a reduction in density.

This apparent inconsistency is probably a surface-related phenomenon. It is considered that density suppression is a result of thin B_2O_3 surface films on the B_4C or trace oxidizing species in the sintering gas which produce volatile boron oxides that coat the Al_2O_3 particle surfaces forming a liquid phase and, thus, premature reduction in surface activity of the Al_2O_3 powder and loss in sinterability. As the sintering temperature increases, the ionic diffusivities increase and at temperatures above ~ 1600° C, mobilities become high enough to cause enhanced densification, and significant increases in density are observed.

Diffusion couple experiments at temperatures up to 1850° C in purified argon did not show evidence of any B_4C–Al_2O_3 interaction, implying that tramp oxygen impurity is the likely cause of the observations. Certainly, thermodynamic calculations indicate no chemical reaction between B_4C and Al_2O_3 (Table II) in the absence of impurities due to the high stability of Al_2O_3.

Boron carbide is unstable at high temperatures in the presence of moisture, oxygen and nitrogen, which explains the deterioration of the pellets using atmospheres other than argon. Boron nitride is more stable than the carbide at all temperatures and the reaction is kinetically controlled, becoming important above 750° C. Loss of boron became significant above 1400° C indicating formation of volatile species. In a hydrogen environment no reaction is expected other than reduction of the surface oxide film but traces of oxygen or moisture cause progressively more rapid oxidation of the B_4C with increase in temperature. However, in reducing atmospheres and also vacuum the volatility of Al_2O_3 suboxides increases, particularly in the presence of water vapour [3, 4], which

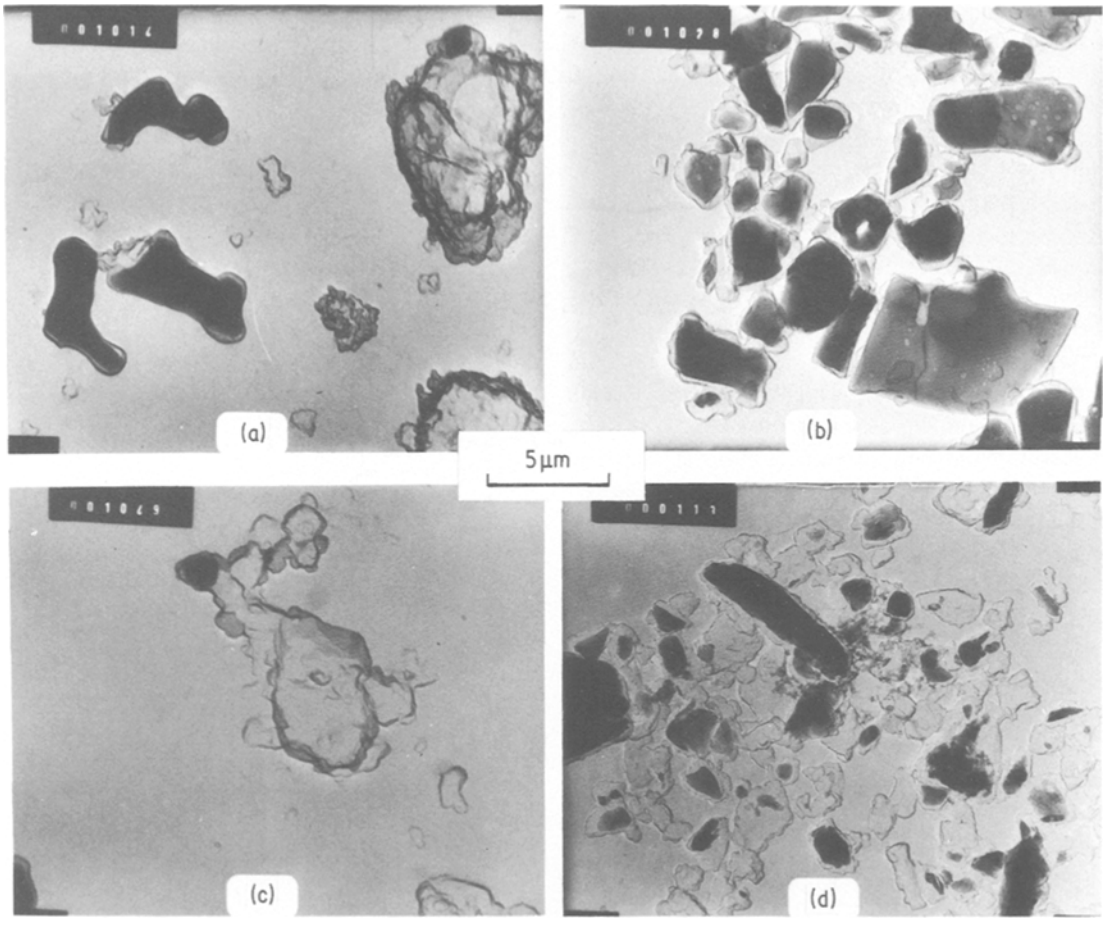

Figure 10 Carbon replica transmission electron micrographs of Al_2O_3 powders: (a) type 9; (b) type 4; (c) type 6; (d) type 10.

induces a more reactive environment for the B_4C thereby deteriorating the material further, as shown by Reactions 10 and 11 listed in Table II.

Time does not appear to be a significant variable in the sintering of these composites. Some loss in density was noted with extended sintering times at temperatures of 1600° C and above, which may be due to progressive oxidation in the presence of tramp oxygen. Maximum pellet density is achieved essentially immediately on attaining the sintering temperature, with little apparent change thereafter.

Microstructural development is consistent with the particle size of the B_4C, the sintering activity of the Al_2O_3 powder and the sintering temperature. However, marked differences are found in location and size of the porosity for Al_2O_3 powders from different suppliers. At low densities (< 75% TD) the Alcoa and Norton Al_2O_3 powders tend to shrink away from the B_4C particles during sintering, providing numerous coarse ($> 10\,\mu m$) as well as fine ($> 1\,\mu m$) pores whereas the Reynolds and Linde powders tend to form only fine pores ($\leqslant 1\,\mu m$). With increased pellet density, many of the coarser pores are removed, but the finer pores tend to remain. At densities ~ 85% TD consolidation of the finer pores occurs giving pores 2 to $3\,\mu m$ in size, with these being reduced in number as the sintering temperature and density increase.

Although a reasonable dependence of pellet density with Al_2O_3 particle size is observed (Fig. 6), differences between powder types are clearly illustrated in Fig. 7. The surface area, which traditionally is a measure of powder activity, is an insufficient parameter to characterize the sinterability of the Al_2O_3 powders although linear dependencies are seen for powders from

two suppliers. In addition, the response changes with higher surface-area B_4C powder (Fig. 5), in the absence of sinterability differences between different Al_2O_3 powders; this may, however, be due to the greater density-inhibiting effect of the finer B_4C.

To explain these observed differences, replica TEM studies on four Al_2O_3 powders were performed. Representative photomicrographs are shown in Fig. 10. The most obvious difference between the powders was the ease of dissolution in preparing the replicas. The A16 powder could not be dissolved after prolonged acid and alkali attack, whereas the others dissolved more readily, indicating significant differences in surface activity. However, enough dissolution at the edges occurred to show that this powder had the smoothest surface, whereas the others showed very irregular particles with multiple facets. The Linde A powder was observed to be composed of two types of particles, with one smooth and not readily dissolved, and one irregular in shape and easily dissolved. All powders showed particles in the same size range, and although qualitative differences can be seen between these powders, causes for the observed differences in composite sinterability cannot be defined.

5. Conclusions

Boron carbide suppresses the sinterability of Al_2O_3 powder substantially, and in direct relation to its surface area. Increasing activity of Al_2O_3 powder produces higher sintered densities, in general, but different relationships are observed for different types of powder. A marked increase in sintered density of the composites occurs for temperatures $\geqslant 1700^\circ$ C.

References

1. W. K. ANDERSON and J. S. THEILACKER, "Neutron Absorber Materials for Reactor Control" USAEC, Naval Reactors Handbook (1962).
2. R. J. BURIAN, E. O. FROMM and J. E. GATES, "Effect of High Boron Burnups on B_4C and ZrB_2 Dispersions in Al_2O_3 and Zircaloy-2" BMI-1627, April (1963).
3. W. H. GITZEN, *Amer. Ceram. Soc.* (1970) 130.
4. O. KUBASCHEWSKI, E. LL. EVANS and C. B. ALCOCK, "Metallurgical Thermochemistry" (Pergamon Press, London, 1967) p. 192.

Received 21 June
and accepted 12 July 1982